Sequential Processing of Human ProIL-1β by Caspase-1 and Subsequent Folding Determined by a Combined *In Vitro* and *In Silico* Approach

Peter W. Swaan,[1,4–6] Daren L. Knoell,[2,3,5] Freek Helsper,[1] and Mark D. Wewers[3,5]

Received January 25, 2001; accepted May 3, 2001

Purpose. Interleukin-1β is a multifunctional cytokine produced by activated monocytes and macrophages that requires caspase-1 (IL-1 converting enzyme/ICE) to process the 31kDa inactive precursor protein to the biologically active 17kDa peptide. This activation event involves ICE cleavage at Asp^{27} (site 1) and Asp^{116} (site 2). To address the sequential processing at ICE cut sites we combined *in vitro* analysis and molecular modeling to investigate the sequence of molecular events.

Methods. Pulse chase labeling followed by immunoprecipitation of IL-1β in activated human monocyte lysates demonstrated sequential cutting by ICE at site 1 before site 2 *in vitro*. To corroborate these findings, we constructed a homology model of proIL-1β after the crystal structure of another ICE substrate, human α1-antitrypsin (23% sequence identity).

Results. Comparative modeling revealed that site 1 on proIL-1β is accessible to ICE but site 2 is not. Molecular dynamics simulations following ICE cleavage at site 1 and removal of the 3kDa amino-terminal fragment, rendered site 2 accessible to ICE.

Conclusions. The close agreement between the *in vitro* and modeled behavior of IL-1β support our contention that IL-1β may be structurally related to α1-antitrypsin and also predicts that proIL-1β requires sequential processing for activation. These findings may facilitate the development of novel pharmacological agents that control posttranslational proIL-1β modification, thereby preventing excessive production of this potent inflammatory cytokine.

KEY WORDS: cytokines; inflammation; protein folding; comparative modeling; molecular dynamics.

INTRODUCTION

Interleukin-1β (IL-1β) is a 17 kDa multifunctional pro-inflammatory cytokine that has effects on nearly every cell type (1). Unlike most inflammatory molecules it lacks a signal sequence to direct its secretion (2). The most important regulatory step requires proteolytic activation by caspase-1 and subsequent release by an as yet uncharacterized pathway. In this context, very little is known about the initial events that regulate converson of proIL-1β by caspase-1.

Mononuclear cells require transcriptional activation to synthesize the 31 kDa proIL-1β molecule. The precursor molecule has limited activity and is synthesized in the cytosolic compartment where caspase-1 (IL-1β converting enzyme, ICE) also resides in an inactive form (3). Despite significant interest in therapeutically controlling the post-translational modification of proIL-1β, there is no information regarding the molecular conformation of proIL-1β. Furthermore, the exact sequence of molecular events that precede mature IL-1β release is unknown. Based on this, characterization of the three-dimensional structure of proIL-1β would assist in directing experimental strategies to dissect key cytosolic processing and export pathways.

The crystallographic structure of mature IL-1β and the active caspase-1 complex have been identified whereas the structure of proIL-1β remains unknown (4,5). Mature IL-1β exists as a very stable pyramidal structure featuring a β-barrel topology composed of 12 antiparallel β-strands, with a core containing hydrophobic side chains. Its two distinct points of contact with the putative signaling receptor, interleukin-1 type I receptor (IL-1RI), have been characterized by X-ray crystallography and site-directed mutagenesis (6,7). It has previously been suggested that proIL-1β exists in a loosely folded conformation compared to the protease insensitive mature form (8). Structure-function mapping of IL-1 precursors following limited proteolysis indicates that significant conformational changes occur prior to packaging of the mature protein (8). This suggests that access to key protein domains change during transition from proIL-1β to mature IL-1β and may be necessary for interactions with yet to be identified release related molecules. In support of this, mature IL-1β is the dominant species released by activated macrophages and is linked to ICE processing. ProIL-1β release occurs to a lesser extent in activated cells (3,9).

We are the first to demonstrate that proIL-1β has significant amino acid homology to α1-antitrypsin (α1-AT). Based on this observation we developed a structural model of proIL-1β based on the crystal structure of uncleaved α1-AT. To validate the homology model, we compared *in vitro* patterns of ICE cleavage to the modeled structure(s) of proIL-1β. Attention was directed at the accessibility of the ICE cut sites, structural stability before and after independent cleavage at the ICE cleavage sites, the anatomical location of the IL-1 RI binding domains in proIL-1β, and comparison to previously reported structure-function mapping. Prior to this we assumed that cut site 1 occurs between Asp^{27} and Gly^{28}; cut site 2 occurs between Asp^{116} and Ala^{117} and that cut site 2 is required to generate the 17 kDa functional form of IL-1β. Our homology model of proIL-1β provides unique information about the structure and function of proIL-1β that has not been previously recognized. The model suggests a structural role for the 11 kDa segment (between cut site 1 and 2) prior to ICE cutting at site 2 and final folding of mature IL-1β. More important, the model explains a requirement for initial

[1] Division of Pharmaceutics, College of Pharmacy, The Ohio State University, Columbus, Ohio 43210.
[2] Division of Pharmacy Practice, College of Pharmacy, The Ohio State University, Columbus, Ohio 43210.
[3] Division of Pulmonary Medicine, College of Medicine and Public Health, The Ohio State University, Columbus, Ohio 43210.
[4] Ohio State Biophysics Program and the HLRI Bioinformatics and Computational Biology Core Laboratory, The Ohio State University, Columbus, Ohio 43210.
[5] Dorothy M. Davis Heart & Lung Research Institute (HLRI), The Ohio State University, Columbus, Ohio 43210.
[6] To whom correspondence should be addressed at College of Pharmacy, 500 West 12th Avenue, Columbus, Ohio 43210-1291. (e-mail: swaan.1@osu.edu)

ABBREVIATIONS: IL-1β, interleukin-1β; α1-AT, alpha 1-antitrypsin; ICE, interleukin-1 converting enzyme; IL-1RI, IL-1 receptor; MD, molecular dynamics.

0724-8741/01/0800-1083$19.50/0

processing at ICE cut site 1 and provides a structural explanation for the weak affinity of proIL-1β to the type I IL-1 receptor.

MATERIALS AND METHODS

Monocyte Purification and IL-1β Production

Peripheral blood mononuclear cells (PBMC) were purified from normal, healthy volunteers. Heparinized (heparin sodium 15 U/ml, Elkins-Shinn, Inc., Cherry Hill, NJ) blood was obtained (60 ml), and PBMC were purified using polysucrose/sodium diatrizoate (Histopaque, Sigma Diagnostics, St. Louis, MO) density gradient centrifugation. The PBMC were counted, washed, and resuspended at a concentration of $5 \cdot 10^6$/ml in RPMI 1640 (BioWhitaker, Walkersville, MD)/5% fetal bovine serum (Hyclone, Logan, UT). By flow cytometry analysis, the composition of the PBMC consisted of approximately 20% monocytes and 80% lymphocytes.

[^{35}S]-Methionine Labeling

ProIL-1β preparations were metabolically labeled with [^{35}S]-methionine by culturing PBMC in methionine-free RPMI 1640 with 10 μg/ml endotoxin (lipopolysaccharide W, E. coli 102F:B8, Difco, Detroit, MI) and the addition of 0.5 μCi/ml [^{35}S]-methionine (Amersham, Arlington Heights, IL). Cells were harvested after 18h and prepared for immunoprecipitation. Cells were lysed in a buffer containing 10 mM Tris, pH 7.4, 1% Nonidet P40 (Sigma), leupeptin 1 μg/ml, pepstatin 1 μg/ml, EDTA 1 mM, and methoxysuccinyl-Ala-Ala-Pro-Val chloromethylketone. Lysates were cleared of nuclei and cell particulates by centrifugation at 1,000*g*. This material was used for later purification and ICE cutting experiments. Purification of proIL-1β Lysates were buffered to pH 8.0 with 1M Tris and incubated with either carboxyterminus-specific or aminoterminus-specific rabbit antisera to human IL-1β; at a 1:100 dilution at 4°C for 1h (9). Immunoglobulin complexed material was incubated with protein A Sepharose (Bio-Rad Laboratories, Hercules, CA) for 1h and unbound material removed by washing three times with PBS. The beads were eluted with 100 mM glycine buffer pH 3.0 and the eluate immediately buffered to pH 7 with 1M Tris.

IL-1β Converting Enzyme (ICE) Processing of proIL-1β

The ability of proIL-1β to be processed by ICE was evaluated by incubating immunoaffinity purified [^{35}S]-methionine labeled proIL-1β with 5 U of functional recombinant ICE (gift of Nancy Thornberry and Doug Miller, Merck Research Laboratories, Rahway, NJ) in 25 μl volume of processing buffer (50 mM HEPES pH 7.5, 10% sucrose, 0.1% CHAPS, 2 mM DTT) for 2 h at 30°C. Proteolysis was stopped by the addition of 1 mM iodoacetate. Processed proIL-1β was evaluated by subsequent SDS polyacrylamide gel electrophoresis and autoradiography.

In Vitro IL-1β Processing

In separate experiments PMBC were evaluated for cell mediated proIL-1β processing. PBMC were cultured with LPS (10 ug/ml) for 1h in complete media (RPMI 1640, 5%FBS, gentamicin 50 ug/ml) and then for 2h in methionine depleted RPMI 1640, 5% FBS, gentamicin. Cells were then pulsed with [^{35}S]-methionine (0.5 μCi/ml) for 1h. Free methionine was washed from the adherent cells and cells cultured in complete media for 2, 4, and 20h. At these time points cell supernatants were harvested and cell lysates were obtained as mentioned above. Supernatants and lysates were immunoprecipitated with either a carboxyterminus-specific rabbit polyclonal antibody (generated against recombinant 17 kDa IL-1β) or an aminoterminus specific rabbit polyclonal antibody (generated against a peptide representing amino acids 3-21 from proIL-1β) as previously described (10). Samples were eluted from protein A beads by boiling in Laemmli sample buffer before analysis by SDS-PAGE, gel drying and autoradiography.

Model Building

Modeling was carried out on a Silicon Graphics O2 with Sybyl (v6.5.3, Tripos, Inc. St. Louis, MO) using the Tripos force field at a constant dielectric function (ε 4.0) and a nonbonded cutoff distance of 8.0Å. An initial protein BLAST search with proIL-1β (11) at EMBL (www.embl.org) using the WU-BLAST routine detected high-scoring segment sequences for IL-1β (P[N] = 4.5e-123), serine protease cleaved α1-AT (P[N] = 3.8e-09) and uncleaved α1-AT (P[N] = 1.5e-05). Because of our interest in a model for proIL-1β, the uncleaved form of α1-AT was further analyzed revealing a high score of 136 amino acid residues combined with 32% identity and 48% positives. An alignment between the sequences of proIL-1β and uncleaved α1-AT was calculated with ClustalW-routine (v1.74) (12) using the BLOSUM80 weight matrix (12). The alignment was analyzed with MPSA (13) (Fig. 3). ProIL-1β and uncleaved α1-AT share 23% sequence identity, 23% strong amino acid similarity, and 16% weak similarity, with an overall shared homology of 62% (Fig. 3). This was verified by MULTALIN (14) at PBIL using default parameters and the BLOSUM62 algorithm, demonstrated 67% significantly conserved residues between the two molecules. The crystal structure of uncleaved α1-AT (PDB entry ID#1ATU (15) at 2.7Å resolution) was used as a scaffold for comparative modeling of proIL-1β using MODELLER4 (16). Its CHECK_ALIGNMENT routine was used to verify internal consistency of the alignment input file. A homology model was exported in PDB format and examined for structural errors using PROCHECK (17).

Molecular Dynamics (MD)

The proIL-1β molecule was centered in a lattice box extending 5Å beyond the molecule's dimensions. Periodic boundary conditions were used and a water solvation shell with mobile counterions was added using the Silverwater algorithm. All atoms were position restrained with a harmonic constant of 90 kJ/mol·Å2 and the energy was minimized to convergence, i.e., <0.01 kJ/mol change in potential energy between two successive iterations. Subsequently, atoms were freed of any constraints and energy was further minimized. The resulting structure was used as a starting configuration for the computation of MD trajectories.

MD simulations (MDS) were performed with the internal force field. Except for aromatic side chains, non-polar hydrogen atoms were excluded in calculations and treated by

the united-atoms approach. Polar residues were assumed to be in the charged state corresponding to the intracellular cytosolic pH (7.2). Bond lengths were constrained by the SHAKE algorithm with a 2.0fs integration time. The twin-range method was used to treat non-bonded interactions (18) with short-range and long-range cut-off radii of 8.0 Å and 1.4 Å, respectively. Initial atomic velocities were assigned from a Maxwell distribution at 300K and the temperature was gradually raised to 500K within 25 ps. Thereafter, the system was kept at constant temperature for an additional 100 ns (heating/cooling rate 1.0 kcal/atom·fs).

RESULTS

In Vitro Processing of ProIL-1β by ICE

The naturally processed forms of IL-1β were evaluated to determine the potential sequence with which the two known ICE cleavage sites are used *in vitro*. Fig. 1 demonstrates the forms generated when native human monocyte-derived proIL-1β is processed *in vitro* with recombinant ICE. Our results show that the generated fragments were a consequence of cleavage at ICE site 1 alone (generating 28 kDa and 3 kDa fragments) or ICE site 1 and 2 together (generating 11 kDa and 17 kDa fragments) but importantly, there was no evidence demonstrating cleavage at ICE site 2 alone (which should generate a 14 kDa fragment). This suggests that ICE cut site 2 requires prior cleavage at site 1.

To document that this is not an artifact of *in vitro* processing and to better characterize the specificity of the cleaved fragments, we evaluated the cleaved forms of IL-1β in monocytes actively processing and releasing IL-1β in response to endotoxin. A pulse chase approach demonstrates a pattern (Fig. 2) similar to the *in vitro* processing shown in Fig. 1. The carboxyterminus specific antibody detects the 31, 28 and 17 kDa fragments in both cell associated and released fractions, as expected. The aminoterminus specific antibody detects the 31 and 3 kDa fragments but fails to detect a 14 kDa fragment that would be expected if there were cleavage at ICE site 2 alone. Together these data demonstrate that proIL-1β cleavage can occur at ICE site 1 without cleavage at ICE site 2. Furthermore, cleavage at ICE site 2 does not occur without prior processing at ICE site 1.

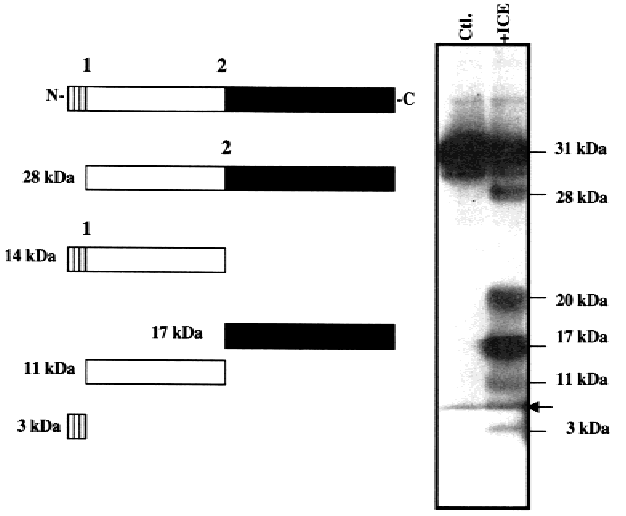

Fig. 1. *In vitro* ICE processing of proIL-1β. The forms of IL-1β generated by subjecting affinity purified native proIL-1β to ICE cleavage are shown. The left side shows the expected cleavage sites on proIL-1β with "1" representing the first cleavage site, Asp 27, and "2" representing the second cleavage site, Asp 116. The hatched segment represents the 3 kDa aminoterminal sequence before Asp 27, the open segment represents the 11 kDa segment between the two cut sits and the filled segment represents the carboxyterminal 17 kDa functional form of IL-1β. Shown are the potential forms that could be generated. The right side shows the actual forms generated by subjecting affinity purified [^{35}S]-methionine labeled proIL-1β to recombinant ICE . The arrow shows the dye front of the gel.

A Homology Model of ProIL-1β

The final model (Fig. 4B) is shown with reference to the crystal structure of α1-AT (Fig. 4A) to illustrate the spatial arrangement of the IL-1β amino acid residues in proIL-1β prior to cleavage by caspase-1. Interestingly, a protein segment of mature IL-1β is trapped within the protein core of proIL-1β (46 residues, Ile^{172}–Asn^{218}; proIL-1β residue numbering, henceforth named "trapped loop") and requires refolding after cleavage by ICE to form the biologically active conformation.

It is presently not known what prevents proIL-1β from triggering the type I IL-1 receptor. The "trapped loop" concept provides a potential explanation because it implies that processing by ICE allows refolding to occur. In support of the "trapped loop/refolding" concept we modeled the receptor binding sites of our model of proIL-1β with mature IL-1β. We highlighted the amino acids in proIL-1β comprising the putative binding domains I and II recognized by the IL-1RI (6) (Figs. 4C and D). Our model demonstrates that the amino acids comprising binding domain I are clustered in an array similar to mature IL-1β, whereas the amino acids associated with domain II are dispersed throughout proIL-1β. The

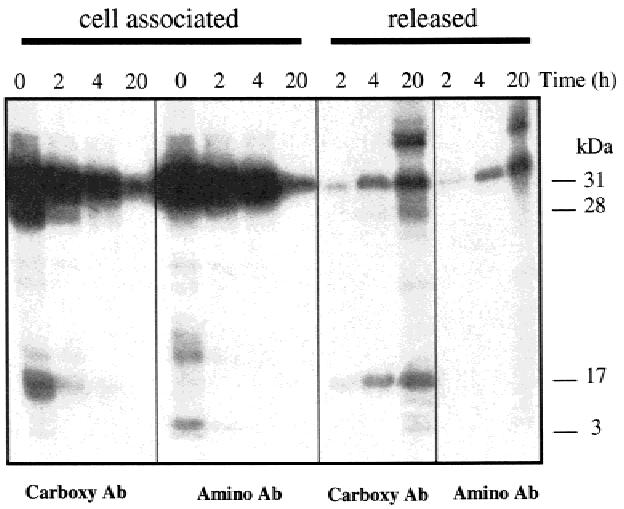

Fig. 2. *In vitro* processing of proIL-1β. The forms of IL-1β generated by human monocytes in culture were analyzed by [^{35}S]-methionine pulse chase experiments. Samples (*cell associated,* i.e., lysates, and *released,* i.e., supernatants) were subjected to immunoprecipitation with either a carboxyterminus or aminoterminus specific antibody and protein A beads. Beads were washed in PBS and then mixed in Laemmli sample buffer, boiled and subjected to gel electrophoresis with SDS 10% polyacrylamide. Gels were dried and analyzed by autoradiography.

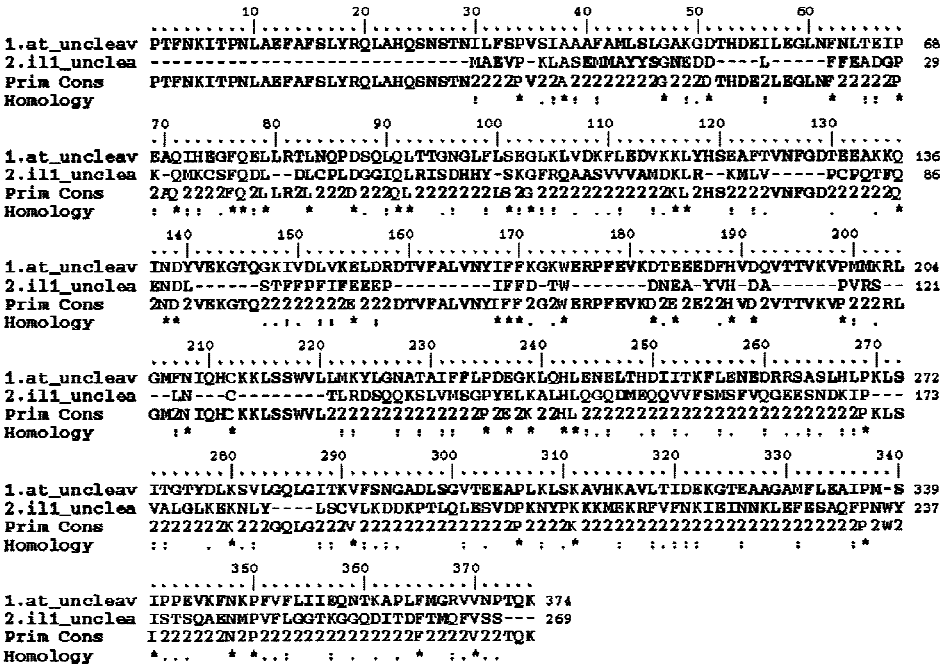

Fig. 3. PSA alignment between α1-AT (*1.at_uncleav*) and ProIL-1β (*2.il_uncleav*). The bottom row shows total sequence homology displaying 23% sequence identity (*), 23% high similarity (:), and 16% low similarity (.), with an overall shared homology of 62%.

model suggests that as proIL-1β is sequentially processed by ICE, the amino acids of binding domain II aggregate thereby significantly increasing the affinity of IL-1β for the IL-1RI and biological activity of the molecule (Figs. 4C and D). Our functional explanation is supported by previous data demonstrating that in comparison to mature IL-1β, proIL-1β has weak affinity for the IL-1 RI resulting in marginal cell activation (19).

Further support for our model is provided by comparing the solvent accessibility of cysteine residues in proIL-1β to those in the crystal structure of mature IL-1β. Hazuda and colleagues previously identified four cysteines within proIL-1β that were biochemically reactive (8). In contrast, the two cysteine residues retained by mature IL-1β are not reactive and are not involved in disulfide bridges (20). They concluded that proIL-1β has a more exposed, protease sensitive tertiary structure in comparison to mature IL-1β. Our model strongly supports these findings (Figs. 4E and 4F). The model predicts that 4 of 5 cysteine residues in proIL-1β are exposed to the outside environment (>25% accessibility) whereas the two cysteines of mature IL-1β are embedded within the hydrophobic core with very limited accessibility (~2%, Table I). Lastly, we inspected the solvent accessibility of the two known ICE cleavage sites (Table II), which reveals that cut site 1 is located at the surface of the protein, whereas cut site 2 is presumably buried within the protein core. Thus, our proIL-1β model supports the *in vitro* observation that a 14 kDa protein fragment generated by a single cut of ICE at cleavage site 2 cannot occur.

Artificial Cleavage of a 3kDa Fragment at Cut Site 1

ICE activity between Asp^{27} and Gly^{28} was simulated by removing a 27 amino acid 3kDa protein fragment from the proIL-1β model. The N-terminus of the novel protein was rectified to an amine moiety by adding a hydrogen atom. An energy minimization was performed to ensure relaxation of the N-terminal domain. Subsequently, the molecule was subjected to a 50ns MDS. Snapshots were collected every 10ps and conformations representing essential structural movements are illustrated in Fig. 4G (top row). The collective movements indicate a high degree of freedom of the protein segment proximal to the second ICE cut site. Over the time interval studied this second cut site becomes accessible, presumably for caspase-1, as reflected by the change in solvent accessibility (Table 2). Interestingly, a distinct portion of the molecule (amino acid 116–171 and 219–269) remains in a relatively rigid conformation evidenced by a low degree of kinetic energy (data not shown). This part of the molecule consists of six stable β-barrels that flank the hydrophobic core of mature IL-1β

Although a higher global solvent accessibility is expected after MDS, Table 2 clearly illustrates that the second cleavage site has a higher accessibility when compared to a control 25 ns simulation with native proIL-1β. Indeed, the deviation from the homology model observed during simulations was not distributed uniformly along the sequence. The largest changes occurred in the 11 kDa region of the molecule and occurred rather quickly after the start of the simulation (200 ps). This deviation from the native structure serves as an indicator of where the molecule is most likely to unfold. Our model suggests that proteolysis takes place during the unfolding of the 11 kDa fragment by a concerted interaction between caspase-1 and proIL-1β at cut site 2.

Sequential Cleavage of an 11kDa Fragment at Cut Site 2

The second ICE cut site was simulated by sequentially removing the 11 kDa protein fragment from the above product, thereby essentially liberating the trapped loop. The resulting molecule was subjected to an identical MD protocol and snapshots of representative conformations are shown in

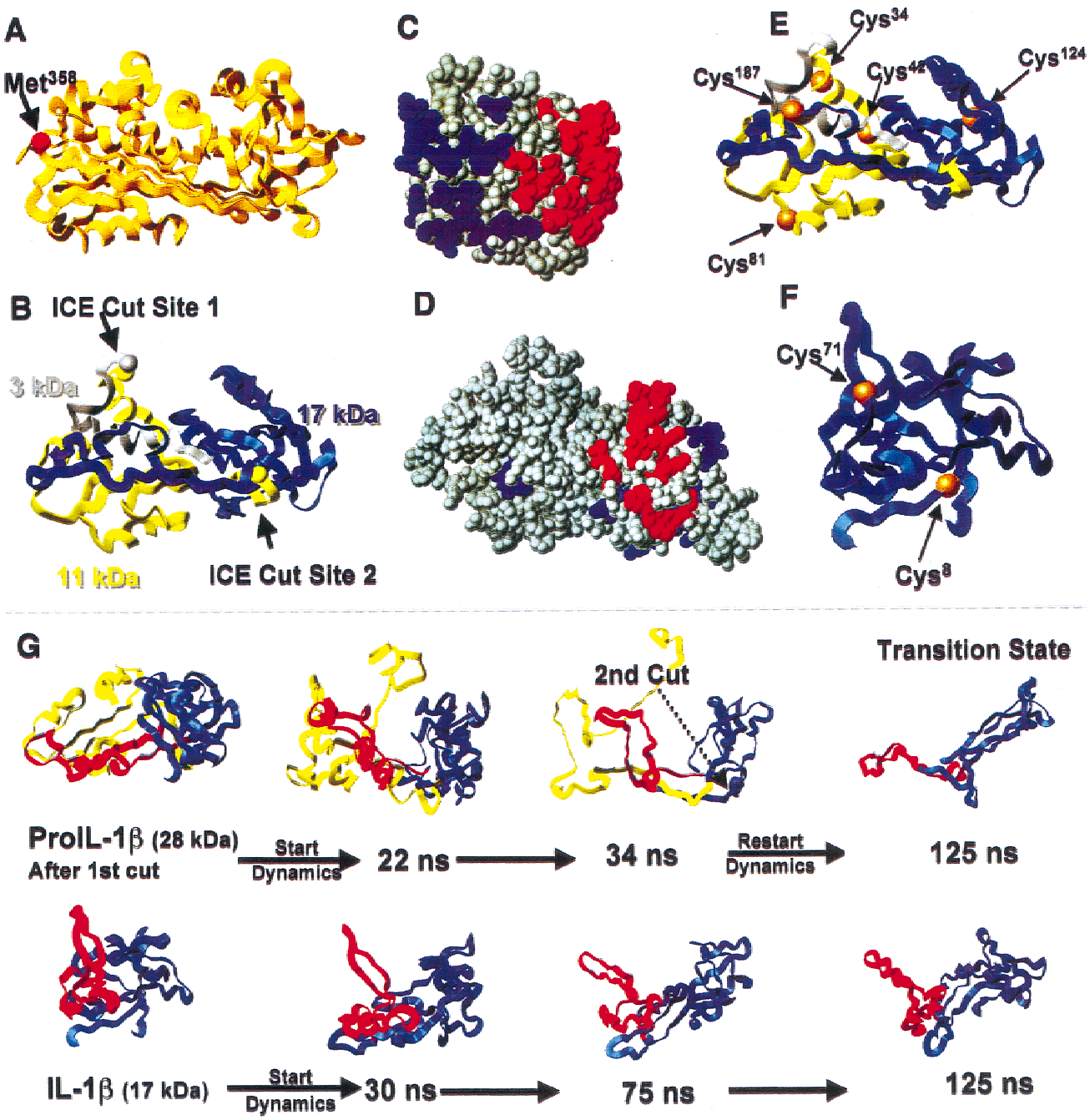

Fig. 4. Crystal structure of (A) α1-AT and a homology model of (B) ProIL-1β based on (A). The α1-AT neutrophil elastase binding site (Met^{358}) residue is given in red. Significant ICE target residues and resulting protein fragments in ProIL-1β are coded: the 3 kDa fragment resulting from proteolytic cleavage at cut site 1 (gray), the 11 kDa fragment following sequential cutting at site 2 (yellow), the 17 kDa mature IL-1β fragment (blue). Cut sites are visualized by spheres. Distribution of IL-1RI receptor binding sites in mature IL-1β (C) and proIL-1β (D). Amino acid residues comprising binding site 1 (red) and binding site 2 (blue) are visualized in a CPK rendering of the mature and pro-form of IL-1β. This delineates low intrinsic affinity of proIL-1β for the IL-1RI receptor and a requirement for conformational reorientation (i.e., refolding) of the cleaved protein to generate binding site 2. Distribution of Cys residues in (E) the ProIL-1β model and (F) the crystal structure of mature IL-1β. Residues are numbered according to native sequences. Color coding according to Fig. 4B. *G:* Simulations of ProIL-1β unfolding in response to proteolytic action by ICE and mature IL-1β unfolding. Main-chain traces are shown of representative conformations during MD unfolding simulations of proIL1β and IL-1β. Mature IL-1β is shown in blue, with its "trapped loop" annotated in red; the 11 kDa fragment is given in yellow. Simulation on ProIL-1β are started from its α1-AT based homology model after initial removal of the 3 kDa fragment resulting from proteolytic cleavage by ICE (top left). MD simulations are carried out up to 75 ns and the 11 kDa section is removed to simulate the 2^{nd} cleavage by ICE. The resulting molecule is subjected to an additional MD trajectory up to 125 ns resulting in a stable molten globule or transition state. Simultaneous MD simulation of IL-1β unfolding lead to a similar (r.m.s.d. 5.8 Å between the two average final 10 ns trajectories) transition state conformation (lower panel).

Table I. Solvent Accessibility of Cysteine Residues in Mature and ProIL-1β

	Residue	Accessibility (%)[a]
ProIL-1β	Cys^{34}	26.5
	Cys^{42}	55.2
	Cys^{81}	40.4
	Cys^{124}[b]	40.1
	Cys^{187}[c]	9.5
Mature IL-1β	Cys^{8}[b]	1.9
	Cys^{71}[c]	2.1

[a] Solvent accessibility was measured using a 1.4 Å probe in MOLMOL (27).
[b] ProIL-1β Cys^{124} corresponds with IL-1β Cys^{8}.
[c] ProIL-1β Cys^{187} corresponds with IL-1β Cys^{71}.

Fig. 4G. These simulations suggest that the trapped loop is a highly dynamic protein fragment that could enable the formation of a stable transition or putative molten globule state. The next step in this simulation should demonstrate the folding of the transition state conformation into mature IL-1β; however, these studies were not feasible due to computational limitations. Alternatively, we studied the unfolding of mature IL-1β at elevated temperature (423K).

Unfolding of Mature IL-1β

Various proteins have been observed to exist in conformations that are neither fully folded nor unfolded, the so-called molten globule state (21). The study of temperature-induced protein unfolding has a computational advantage in lieu of folding since the simulations proceed from a well-defined starting structure (22). Subjecting the crystal structure conformation of IL-1β (PDB#4I1B@2.0Å resolution) (4) to a molecular dynamics protocol at 423K reveals unfolding of the native state with release of the 'trapped loop' fragment into a transition state (Fig. 4G). The resulting conformation strongly resembles the transition state derived from processed proIL-1β as described above. Interestingly, the trapped loop readily evacuates the IL-1β crystal structure, whereas the remainder maintains its stable conformation. Combining our findings, it becomes conceivable that sequential enzymatic processing of proIL-1β allows refolding into its mature form. Backbone superposition of cleaved proIL-1β and mature IL-1β (using the average conformations over the final 10 ns of each MD simulation) reveals an average r.m.s. α-carbon displacement of approximately 6.8 Å. Based on these data we speculate that the folding of IL-1β from its molten globule state may follow the reverse trajectory of its unfolding pathway.

Table II. Solvent Accessibility of ICE Target Residues

	Residue	Accessibility (%)[a]
ProIL-1β (native state)		
Cut site 1	Ala^{26}	43.0
	Asp^{27}	62.7
Cut site 2	Asp^{116}	5.7
	Ala^{117}	4.0
ProIL-1β (after control MDS)		
Cut site 1	Ala^{26}	62.8
	Asp^{27}	79.2
Cut site 2	Asp^{116}	16.8
	Ala^{117}	9.3
ProIL-1β (-3kDa, after MDS)	Asp^{116}	57.4
	Ala^{117}	58.1

[a] Solvent accessibility was mapped using a 1.4 Å probe atom in MOLMOL (27).

DISCUSSION

Without knowledge of the three dimensional structure of proIL-1β it has been difficult to define the sequence of events that occur during the caspase-1 mediated processing of proIL-1β and its subsequent release from the cell. It is known that the 31 kDa precursor has two caspase-1 cleavage sites and that theoretically, proIL-1β can exist in 6 different forms (31, 28, 17, 14, 11 and 3 kDa), depending on the relative sequence of cleavage at these sites (9). It has clearly been established that the intact 31 kDa precursor is the predominant intracellular form of IL-1β and the 17 kDa mature peptide is the predominant released extracellular form. Schmidt and colleagues as well as our own laboratory (9,23) reported *in vitro* evidence that the 3 kDa fragment is preferentially released following cleavage at site 1 demonstrating that intracellular 31 kDa is initially cleaved to the 28 kDa form. This demonstrates that cleavage at site 1 without cleavage at site 2 does occur *in vitro*. However, there is little supportive *in vitro* evidence that cleavage can occur at site 2 without cleavage at site 1. As mentioned, if cleavage preferentially occurred at site 2 (Asp^{116}), a 14 kDa amino terminal fragment would be generated. Our unique antibody that recognizes the amino terminus region of IL-1β would detect this fragment; however, we and others have been unable to demonstrate its presence. In this context, the predictions provided by the current model provide an explanation for the absence of the 14 kDa fragment since cut site 2 is not accessible until site 1 cleavage occurs.

This report takes advantage of our initial observation that proIL-1β has significant homology with human α1-AT, an extensively studied protein (24) that is also a caspase-1 substrate (data not shown). Since proIL-1β structure has not been characterized we used MODELLER (16) to develop a working model of proIL-1β's structure based on known structure of native α1-AT. We then compared the predicted structure, caspase-1 cleavage sites, receptor binding domains and the effect of cleavage at site 1 and site 2 on the cleavage products and folding dynamics of proIL-1β using an iterative molecular dynamics protocol.

In addition to predicting the spacial relevance of each ICE cut site, the model also provides an explanation for the observed differences in receptor binding affinity between the 31 and 17 kDa molecules. In this regard the modeled structure of the precursor form of IL-1β contains a 46 amino acid "trapped loop" sequence which we believe to be a critical structural component of mature IL-1β that is captured within proIL-1β. According to the model, proteolytic removal of the propiece by ICE cleavage at cut site 2, after cleavage at cut site 1, allows mature IL-1β to become a functionally competent ligand for the IL-1RI. We believe that this occurs when the "trapped loop" domain joins the remainder of the mature molecule thereby appropriately packaging the key receptor

recognition domains and enhancing the affinity of IL-1β for its cognate receptor (6). We also predict that a major function of the aminoterminal 14 kDa and subsequent 11 kDa segments of proIL-1β during processing are to retain IL-1β in a nonfunctional state until final cleavage and exposure of the "trapped loop" occurs.

As described, our model suggests that ICE cut site 1 is exposed in the precursor molecule and ICE cut site 2 is hidden until site 1 cleavage has occurred. Studies by Hubbard and co-workers (25) have shown that proteolysis requires large local motions proximal to scissile bonds; furthermore, the ability to unfold locally without perturbing the overall protein conformation is requisite for proteolysis. Our model is further supported by *in vitro* observations made by our laboratory and others demonstrating that the first major ICE cleavage form of IL-1β is the 28 kDa intracellular precursor associated with the concomitant generation of a 3kDa aminoterminal fragment. As mentioned earlier, there are several potential cleavage products of IL-1β, including a 14 kDa form that would be feasible if proIL-1β could be cleaved at caspase site 2 without prior cleavage at site 1. In this regard, there is experimental data with recombinant proIL-1β that conflicts with our model. It has been shown that cutting at site 2 occurs when recombinant proIL-1β mutated to remove cut site 1 is exposed to ICE (26). In contrast, our homology model of proIL-1β and biologic studies with native proIL-1β indicate that site 2 cleavage does not occur in the absence of site 1 cleavage. It is interesting to speculate that this discrepancy represents differences between recombinant and native proIL-1β structure.

Lastly, the modeling predicts that the cleavage at site 1 generates a structure that contains a highly mobile aminoterminal arm with the subsequent exposure of site 2 to caspase cleavage. The instability of the freshly generated aminoterminal fragment caused by cleavage at site 1 raises the possibility that the folding and refolding that occurs in tandem with caspase-1 cleavage is not likely to take place in the absence of accessory proteins. It is highly probable that chaperonins or related molecules exist that also interact with proIL-1β and its cleaved forms. Since the release of IL-1β from the cytosol occurs by nonconventional means, one can speculate that release related proteins are involved in the export process. In this context, the structural changes predicted by the current model are currently being used in the design of approaches to capture these affiliated molecules responsible for bringing active caspase-1 to precursor proIL-1β and for the export of IL-1β.

In summary, proIL-1β was modeled after the crystal structure of human α1-AT. Indeed, homology modeling revealed that site 1 on the derived structural model of proIL-1β is readily accessible to ICE whereas site 2 is not. This finding corroborates detailed *in vitro* analysis of activated monocyte lysates and supernatants that demonstrate ICE cleaved proIL-1β fragments are preferentially derived by initial cleavage at the Asp27 residue. Furthermore, MDS revealed that removal of the 3 kDa amino terminal fragment was required to expose the second cut site and ultimately generate a 17 kDa fragment capable of refolding into a stable structure resembling mature IL-1β. Combined, our biological and computational data support our hypothesis that proIL-1β requires sequential processing by ICE to generate the biologically active 17 kD mature protein prior to release. These findings may provide useful strategies to design pharmacologically active agents that control IL-1 processing at different steps thereby preventing excessive production of this potent inflammatory cytokine when appropriate.

ACKNOWLEDGMENTS

This work was funded by NIH grants HL40871 (to MDW), HL56336 (to DLK), a Dutch Foundation of Pharmacy (KNMP) travel grant (to FH) and a Pharmaceutical Research and Manufacturers of America Foundation (PhRMAF) New Investigator Grant (to PWS).

REFERENCES

1. C. A. Dinarello. Biologic basis for interleukin-1 in disease. *Blood* **87**:2095–2147 (1996).
2. C. J. March, B. Mosley, A. Larsen, D. P. Cerretti, G. Braedt, V. Price, S. Gillis, C. S. Henney, S. R. Kronheim, and K. Grabstein. Cloning, sequence and expression of two distinct human interleukin-1 complementary DNAs. *Nature* **315**:641–647 (1985).
3. N. A. Thornberry, H. G. Bull, J. R. Calaycay, K. T. Chapman, A. D. Howard, M. J. Kostura, D. K. Miller, S. M. Molineaux, J. R. Weidner, and J. Aunins. A novel heterodimeric cysteine protease is required for interleukin-1 beta processing in monocytes. *Nature* **356**:768–774 (1992).
4. B. Veerapandian, G. L. Gilliland, R. Raag, A. L. Svensson, Y. Masui, Y. Hirai, and T. L. Poulos. Functional implications of interleukin-1 beta based on the three- dimensional structure. *Proteins* **12**:10–23 (1992).
5. K. P. Wilson, J. A. Black, J. A. Thomson, E. E. Kim, J. P. Griffith, M. A. Navia, M. A. Murcko, S. P. Chambers, R. A. Aldape, and S. A. Raybuck. Structure and mechanism of interleukin-1 beta converting enzyme. *Nature* **370**:270–275 (1994).
6. G. P. Vigers, L. J. Anderson, P. Caffes, and B. J. Brandhuber. Crystal structure of the type-I interleukin-1 receptor complexed with interleukin-1beta. *Nature* **386**:190–194 (1997).
7. R. J. Evans, J. Bray, J. D. Childs, G. P. Vigers, B. J. Brandhuber, J. J. Skalicky, R. C. Thompson, and S. P. Eisenberg. Mapping receptor binding sites in interleukin (IL)-1 receptor antagonist and IL-1 beta by site-directed mutagenesis. Identification of a single site in IL-1ra and two sites in IL-1 beta. *J. Biol. Chem.* **270**:11477–11483 (1995).
8. D. J. Hazuda, J. Strickler, P. Simon, and P. R. Young. Structure-function mapping of interleukin 1 precursors. Cleavage leads to a conformational change in the mature protein. *J. Biol. Chem.* **266**: 7081–7086 (1991).
9. M. D. Wewers, A. V. Winnard, and H. A. Dare. Endotoxin-stimulated monocytes release multiple forms of IL-1 beta, including a proIL-1 beta form whose detection is affected by export. *J. Immunol.* **162**:4858–4863 (1999).
10. M. D. Wewers, H. A. Pope, and D. K. Miller. Processing proIL-1 beta decreases detection by a proIL-1 beta specific ELISA but increases detection by a conventional ELISA. *J. Immunol. Methods* **165**:269–278 (1993).
11. S. F. Altschul, W. Gish, W. Miller, E. W. Myers, and D. J. Lipman. Basic local alignment search tool. *J. Mol. Biol*. **215**:403–410 (1990).
12. J. D. Thompson, D. G. Higgins, and T. J. Gibson. CLUSTAL W: Improving the sensitivity of progressive multiple sequence alignment through sequence weighting, position-specific gap penalties and weight matrix choice. *Nucleic Acids Res*. **22**:4673–4680 (1994).
13. C. Combet, C. Blanchet, C. Geourjon, and G. Deleage. NPS@: Network protein sequence analysis. *Trends Biochem. Sci*. **25**:147–150 (2000).
14. F. Corpet. Multiple sequence alignment with hierarchical clustering. *Nucleic Acids Res.* **16**:10881–10890 (1988).
15. S. E. Ryu, H. J. Choi, K. S. Kwon, K. N. Lee, and M. H. Yu. The native strains in the hydrophobic core and flexible reactive loop of a serine protease inhibitor: Crystal structure of an uncleaved alpha1-antitrypsin at 2.7 A. *Structure* **4**:1181–1192 (1996).
16. A. Sali and T. L. Blundell. Comparative protein modelling by

satisfaction of spatial restraints. *J. Mol. Biol*. **234**:779–815 (1993).

17. R. A. Laskowski, J. A. Rullmannn, M. W. MacArthur, R. Kaptein, and J. M. Thornton. AQUA and PROCHECK-NMR: programs for checking the quality of protein structures solved by NMR. *J. Biomol. NMR* **8**:477–486 (1996).
18. H. J. C. Berendsen. Treatment of long-range forces in molecular dynamics. In J. Hermans (ed.), *Molecular Dynamics and Protein Structure*, Polycrystal Books, Western Springs, IL, 1985 pp. 123–125.
19. S. A. Jobling, P. E. Auron, G. Gurka, A. C. Webb, B. McDonald, L. J. Rosenwasser, and L. Gehrke. Biological activity and receptor binding of human prointerleukin-1 beta and subpeptides. *J. Biol. Chem*. **263**:16372–16378 (1988).
20. J. P. Priestle, H. P. Schar, and M. G. Grutter. Crystal structure of the cytokine interleukin-1 beta. *Embo J.* **7**:339–343 (1988).
21. J. J. Ewbank and T. E. Creighton. The molten globule protein conformation probed by disulphide bonds. *Nature* **350**:518–520 (1991).
22. V. Daggett and M. Levitt. Protein unfolding pathways explored through molecular dynamics simulations. *J. Mol. Biol*. **232**:600–619 (1993).
23. J. A. Schmidt and R. Bomford. The processing of interleukin-1 beta studied with antibodies raised against synthetic peptides from the precursor N-terminal region. *Cytokine* **3**:240–245 (1991).
24. R. G. Crystal. Alpha 1-antitrypsin deficiency, emphysema, and liver disease. Genetic basis and strategies for therapy. *J. Clin. Invest*. **85**:1343–1352 (1990).
25. S. J. Hubbard, F. Eisenmenger, and J. M. Thornton. Modeling studies of the change in conformation required for cleavage of limited proteolytic sites. *Protein Sci*. **3**:757–768 (1994).
26. A. D. Howard, M. J. Kostura, N. Thornberry, G. J. Ding, G. Limjuco, J. Weidner, J. P. Salley, K. A. Hogquist, D. D. Chaplin, and R. A. Mumford. IL-1-converting enzyme requires aspartic acid residues for processing of the IL-1 beta precursor at two distinct sites and does not cleave 31- kDa IL-1 alpha. *J. Immunol*. **147**:2964–2969 (1991).
27. R. Koradi, M. Billeter, and K. Wuthrich. MOLMOL: A program for display and analysis of macromolecular structures. *J. Mol. Graph*. **14**:29–32 (1996).